Estimation of time to point of closest approach for collision avoidance and separation systems

Estimation Of Time To Point Of Closest Approach For Collision Avoidance And Separation Systems

James Dunthorne, Wen-Hua Chen and Sarah Dunnett
Loughborough University
Email: j.r.dunthorne@lboro.ac.uk

***Abstract*—This paper proposes a method for estimating the amount of time until the point of closest approach (TPCA) between two aircraft. A range of simple methods which use derivatives to estimate the time to collision are analysed. These methods are only accurate when the angle subtended between the direction of the relative velocity vector, and the bearing of the intruder aircraft, θ, is small. An extended method is developed which calculates the exact TPCA from distance and bearing measurements. Representative levels of Gaussian white noise are introduced to the core equation variables for both the derivative and extended methods. It is found that as we increase the value of θ, the extended method's accuracy increases beyond that of the derivative method. A fusion algorithm is developed to switch between methods and is shown to perform well for a range of conflicts. When the relative velocity between the two aircraft is small, the signal to noise ratio on the relative velocity variable reduces causing large errors to the TPCA estimation. It is therefore concluded that at a certain relative velocity threshold, V_k (dependant on sensor and filter performance) both the derivative and extended TPCA estimation methods would become undesirable as risk estimators. It is suggested that in these situations distance could be better to use since it can be measured directly.**

I. INTRODUCTION

For years the military has been using Unmanned Aerial Vehicles (UAVs) in war-zones around the world for reconnaissance and precision air power. Typically they have been operated within military controlled airspace, which has allowed the incorporation of greater functionality, without all of the regulatory hurdles that are present within the civilian world [1]. It is not beneficial to constrain commercial use of UAVs to segregated airspace as this is very costly and time consuming. In order to fly UAVs in non-segregated airspace, one of the challenges is to develop separation and collision avoidance systems which are able to replicate the ability of a human pilot to perform those functions.

In order to assess the risk of a conflict, collision avoidance systems use a variety of risk estimators. Some of the variables used to assess the risk are easy to measure:

- Rate of change of azimuth [2]
- Distance [3]
- Rate of change of azimuth and Time to collision [4]

Others are more complex:

- Estimated distance between the aircraft at the point of closest approach [5]
- Cost functions calculated from partially observable Markov decision processes [6]

Time to collision provides a quick estimate of the severity of a conflict to a human operator and UAV management system. It has been widely used in the context of timing collision avoidance action [7] as it provides a way of measuring the aircraft's progression through an encounter. This is helpful to both the human pilot and UAV flight management system for detecting safe operation periods such as in [8], for applying decision logic such as the rules of the air [1] and for determining whether the UAV should be operating under command of the human operator or fully autonomously [9].

Time to collision in its definition assumes that a collision is going to happen (i.e. the distance between the aircraft at the point of closest approach is zero). However very rarely is this ever the case. Therefore this paper looks to estimate the precise time to point of closest approach (TPCA), which can describe a range of encounters with varying miss distances.

II. SIMULATION ENVIRONMENT

In order to test methods, a simulation environment is used. The aircraft trajectories are modelled in 2 spatial dimensions, x and y, and it is assumed that the aircraft fly linear trajectories at constant velocities. The next section explains how the aircraft's starting positions are found for any given simplified conflict scenario.

A. Encounter Model

Complex encounter models were developed in [10], however these were deemed to be overly complex for the analysis in this paper. Using the assumptions from the previous section, any conflict scenario can be described in the ownship aircraft's reference frame by a simplified set of parameters:

$$V_A, V_B, \psi_{\angle AB}, d_{MIN}, t_{PCA}, \tag{1}$$

Where V_A and V_B are the ownship and intruder aircraft's respective velocities, $\psi_{\angle AB}$ is the difference between the two aircraft's headings:

$$\psi_{\angle AB} = \psi_B - \psi_A \tag{2}$$

$\psi_{\angle AB}$ is measured between the limits $0 \leq \psi_{\angle AB} \leq 2\pi$

d_{MIN} is the distance between the two aircraft at the point of closest approach and t_{PCA} would be the amount of time in seconds until the point of closest approach. A negative value of t_{PCA} means that the point of closest approach has already happened. d_{MIN} can be positive or negative depending on

which side the intruder passes the ownship aircraft. A value of $d_{MIN} = 0$ signifies a direct collision where if the two aircraft were to be represented by a point in space, those points would share the same point in space at the time $t_{PCA} = 0$.

The 4 variables $V_A, V_B, \psi_{\angle AB}$ and d_{MIN} are used to describe the simplified conflict scenario. t_{PCA} is used to locate the progress of the scenario.

1) Collision Offset: We can combine both aircraft's velocities together to form a relative velocity vector, $\overrightarrow{V_r}$. The point of closest approach always occurs when the ownship and intruder aircraft are positioned perpendicular to the direction of the relative velocity vector [11].

$$\overrightarrow{V_r} = \overrightarrow{V_A} - \overrightarrow{V_B} \tag{3}$$

The direction of $\overrightarrow{V_r}$ can be calculated, and if the ownship aircraft' s heading is taken as the reference, it can be simplified to:

$$\psi_r = \tan^{-1}\left(\frac{-V_B \sin(\psi_{\angle AB})}{V_A - V_B \cos(\psi_{\angle AB})}\right) \tag{4}$$

2) Starting Positions: If we now take the ownship aircraft's position at the point of closest approach to be the origin (0, 0). The starting position of the ownship aircraft can be found simply by integrating its velocity with time, yielding:

$$P_A \begin{pmatrix} x \\ y \end{pmatrix} = \begin{pmatrix} 0 \\ -V_A t_{PCA} \end{pmatrix} \tag{5}$$

The intruders starting location is found by first of all offsetting its position at the point of closest approach by a distance of d_{MIN}, along the heading $\psi_r + \frac{\pi}{2}$ from the origin. Then its velocity vector is integrated from this point back through time to find its starting point as shown in Figure 1.

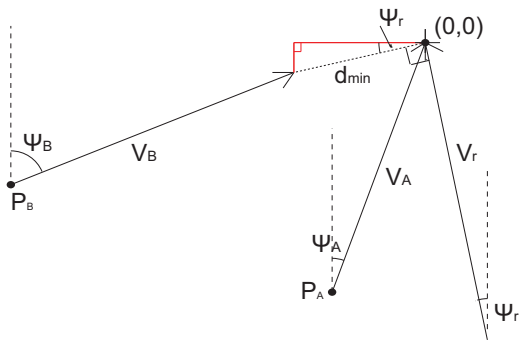

Fig. 1. Derivation of aircraft starting positions

The intruders starting position is expressed as follows:

$$P_B \begin{pmatrix} x \\ y \end{pmatrix} = \begin{pmatrix} -V_B \sin(\psi_{\angle AB}) t_{PCA} - (d_{min} \cos \psi_r) \\ -V_{By} t_{PCA} + (d_{min} \sin \psi_r) \end{pmatrix} \tag{6}$$

B. Kinematic Model

The kinematic model in the simulation is kept very simple since the aircraft do not manoeuvre. The starting positions and scenario data is loaded into the Simulink environment from Matlab. The position of each aircraft at time, t, through the simulation is found by integrating its velocity vector at each time step and adding this to its previous position in the simulation:

$$\overrightarrow{P_{i(t)}} = \overrightarrow{P_{i(t-1)}} + \begin{pmatrix} \int_{t-1}^{t} (V_i \sin(\psi_i))\delta t \\ \int_{t-1}^{t} (V_i \cos(\psi_i))\delta t \end{pmatrix} \tag{7}$$

ψ_i is the heading of aircraft i (i.e. A or B). t and $t-1$ denote the current and previous time steps respectively.

III. Derivative Methods

In [4] it was shown that the point of closest approach can be estimated by dividing the distance to an object by the rate of change of its distance:

$$t_{PCA} = \frac{d}{\frac{\partial d}{\partial t}} \tag{8}$$

d is the distance between the two aircraft (in meters).

For active sensor systems such as radar, measuring distance is not too much of a problem. However passive sensor systems, such as video cameras, struggle to provide accurate distance information. In [12] a method is presented which uses the angular width, α subtended by the intruder aircraft and its rate of change with time to calculate the TPCA.

$$t_{PCA} = \frac{\alpha}{\frac{\partial \alpha}{\partial t}} \tag{9}$$

In [4] this method was extended to take into account the angular area of the intruder in order to help reduce the effect of noise. This new variable, κ, is measured in rad^2.

$$t_{PCA} = \frac{2\kappa}{\frac{\partial \kappa}{\partial t}} \tag{10}$$

All three methods are derived from the same set of equations and in simulation it was found that they all produced identical results for a range of conflicts when uncertainty was ignored. They also all assume that the distance at the point of closest approach is zero. The advantage of using one method over another would be based on the type of sensors being used and the signal to noise ratio on each variable.

A. Limitations

The derivative methods rely on the assumption that the aircraft are involved in a direct collision and so this needs to be tested. The TPCA is calculated using relative information, and so only the these variables are important when testing the algorithms. To keep things consistent, a head-on collision scenario shall be assessed in simulation. Both velocities are set to, $V_A = V_B = 50m/s$, and the difference in headings is $\psi_{\angle AB} = \pi$. The aircraft were set up 10 seconds prior to the point of closest approach, $t_{PCA} = 10$. The distance between

the two aircraft at the point of closest approach, d_{MIN} is increased from $0m$ to $150m$, in $50m$ increments. Each distance is plotted in Figure 2 along with a reference.

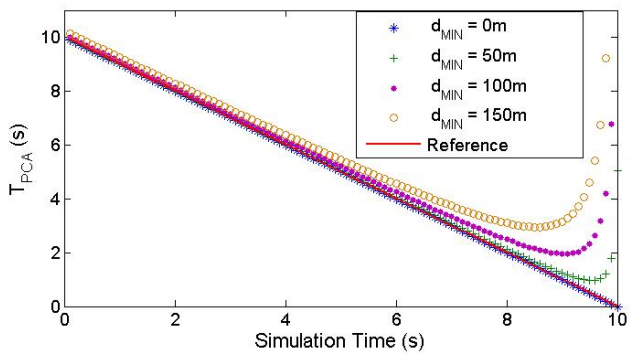

Fig. 2. Derivative method's TPCA prediction for a range of miss distances

As the miss distance d_{MIN} increases, it can be seen that the accuracy of the t_{PCA} estimate reduces, more significantly as the aircraft get closer together. When the aircraft are further apart, d_{MIN} has a negligible effect on the accuracy. If we view the collision in the relative frame of reference, we can see why this inaccuracy is occurring. See Figure 3.

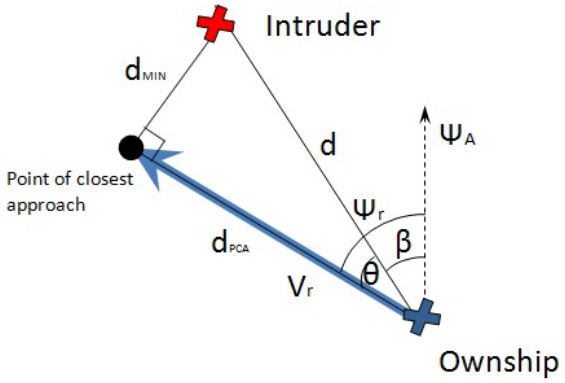

Fig. 3. Derivation of TPCA

β is the difference between the ownship aircraft's heading, and the bearing of the intruder on the ownship aircraft's horizon.

The derivative method described by Equation 8 assumes that the angle, θ is small. Under this assumption, $d \approx d_{PCA}$, and so an accurate estimation is possible.

It was found for angles of $\theta > 10$ degrees, the method would cause noticeable errors. This is not such a problem for a collision avoidance scenarios where $d_{MIN} < 150m$, as accuracy is only lost when the aircraft are very close. For a miss distance $d_{MIN} = 150m$ this occurs with the intruder around 860m away. For a miss distance of $d_{MIN} = 500m$ this occurs with the intruder a distance just over 2.9km away. Figure 4 shows how the error in the derivative method for a miss distance of $d_{MIN} = 500m$.

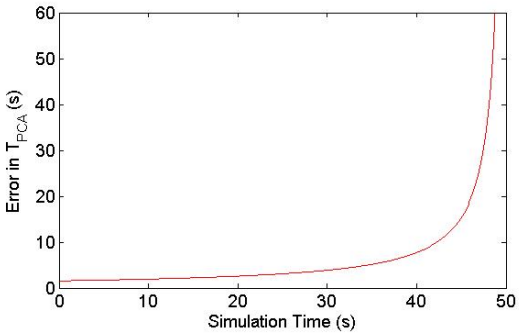

Fig. 4. Error in Derivative TPCA Estimation for large $d_{MIN} = 500m$

It can be seen that the errors increase quite rapidly as the aircraft reach the point of closest approach. Since the TPCA is required for all modes of flight, it was deemed necessary to develop a method to predict the TPCA more accurately in these high θ scenarios.

IV. Extension of Derivative Method

When θ is small it has been shown that the derivative methods introduce very little error. Most of the error is introduced in the form of uncertainty in the measurement. When θ is large, most of the error is caused by the mathematical assumptions breaking down. In these situations it would be necessary to predict the time to point of closest approach more accurately.

If the collision is viewed in the relative frame, where the intruder is stationary, the precise TPCA can be found by dividing the distance to the point of closest approach, d_{PCA}, by the relative velocity, V_r. See Figure 3

$$t_{PCA} = \frac{d_{PCA}}{|V_r|} \tag{11}$$

The variables d_{PCA} and V_r are not easy to measure directly and so need to be calculated.

By deriving things in polar co-ordinates it is found that only the distance, d, the azimuth angle, β as defined in Figure 3, and their derivatives, $\dot{d}$ and $\dot{\beta}$ are needed for the calculation. β is measured between $-\pi$ and π.

A. Relative Velocity

The relative velocity in polar co-ordinates is taken from [13] and stated below:

$$V_r = \dot{d}\hat{e_r} + d\dot{\beta}\hat{e_\beta} \tag{12}$$

Where $\hat{e_r}$ and $\hat{e_\beta}$ are radial and angular unit length vectors. Translating this to Cartesian co-ordinates gives:

$$V_r \begin{pmatrix} x \\ y \end{pmatrix} = \begin{pmatrix} \dot{d}\sin(\beta) - d\dot{\beta}\cos(\beta) \\ \dot{d}\cos(\beta) + d\dot{\beta}\sin(\beta) \end{pmatrix} \tag{13}$$

The magnitude of the relative velocity reduces to:

$$|V_r| = \sqrt{\dot{d}^2 + d^2\dot{\beta}^2} \tag{14}$$

B. Distance to Point of Closest Approach

Now that the magnitude of the relative velocity vector is known, the distance to the point of closest approach must be found. From Figure 3 we know that:

$$d_{PCA} = d\cos(\theta) \tag{15}$$

Where

$$\theta = \psi_r - \beta \tag{16}$$

ψ_r is calculated by finding the arctangent of the x and y components of the relative velocity:

$$\psi_r = \arctan^{-1}\left(\frac{-\dot{d}\sin(\beta) + d\dot{\beta}\cos(\beta)}{-\dot{d}\cos(\beta) - d\dot{\beta}\sin(\beta)}\right) \tag{17}$$

This was tested for the same scenario as in Figure 4, at this stage with no uncertainty added. The results are given in Figure 5.

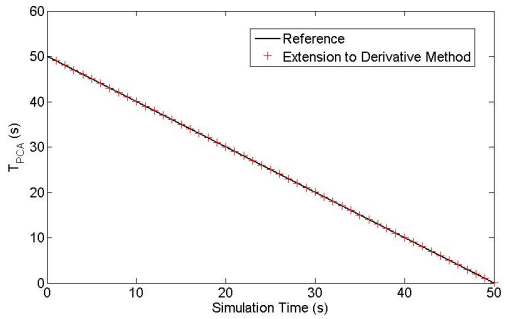

Fig. 5. Extended TPCA estimation method results

It can be seen that this method predicts the TPCA precisely. No mathematical error is introduced.

V. Introduction of Uncertainty

Error is introduced to a signal in 2 ways:

1) Through error made by mathematical approximations and assumptions
2) Through sensor uncertainty being propagated through the maths.

Derivative methods use small angle approximations which cause errors for large values of θ. Error is also introduced by propagation of sensor uncertainty in the maths. The total error is a combination of the error derived from the mathematical approximations and the propagation of sensor uncertainty.

The extended method has been shown to predict the TPCA precisely. Error is only introduced by the propagation of sensor uncertainty through the maths. Since the maths is more complex for the extended method, the uncertainty introduced in this way is likely to be larger.

Uncertainty is introduced to the variables in the core equations. i.e. Equations 8 and 11. Introducing uncertainty in the low level variables such as β and $\dot{\beta}$ would require filtering techniques to be introduced to reduce noise at each stage of the calculation. Sensors will introduce different levels of noise, and engineers will use different types of filters, so quantifying noise at this level would be fairly insignificant.

The propagation of sensor uncertainty is almost always going to be greater on the variable d_{PCA}, than on d which can be measured directly. The same is true, that the propagated sensor error on $|V_r|$, is likely to be greater than on $\frac{\partial d}{\partial t}$. Therefore in all simulations, twice as much error is introduced to the extended method variables. This assumption will allow general trends to be found in the two methods.

The shape and size of the uncertainty is unknown, so realistic levels are introduced in the form of Gaussian white noise. This uncertainty is added to all core variables with standard deviations as shown in Table I. The standard deviations of d_{PCA} and $|V_r|$ are double that of d and $\frac{\delta d}{\delta t}$ for the reasons mentioned above.

TABLE I
Error Distributions

Variable Name	Error Standard Deviation, σ
d_{PCA}	10m
$\lvert V_r \rvert$	4m/s
d	5m
$\frac{\delta d}{\delta t}$	2m/s

A. Error Analysis

A head-on encounter is simulated. $V_A = 40m/s$ $V_B = 40m/s$, $\psi_{\angle AB} = 180°$ and $d_{MIN} = 150m$. Figure 6 shows the total error on both the derivative and the extended methods for this simulation scenario.

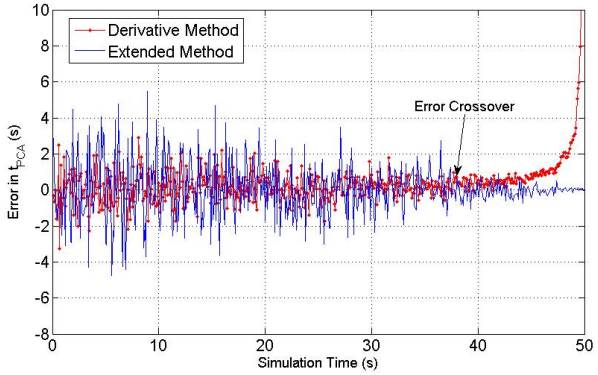

Fig. 6. Error in TPCA estimation for both methods

It can be seen that when the aircraft are further apart and θ is small, the derivative method gives a better prediction of the TPCA with less noise. However as θ increases the errors in the derivative method build up until "Error Crossover" is reached. At this point it becomes better to use the extended method for TPCA estimations. An algorithm was needed which could fuse the two methods together based on the value of θ.

VI. Data Fusion Algorithm

In order to switch between the methods a simple data fusion algorithm is used. It fuses the output of the two methods based on the value of θ, as shown in Figure 7.

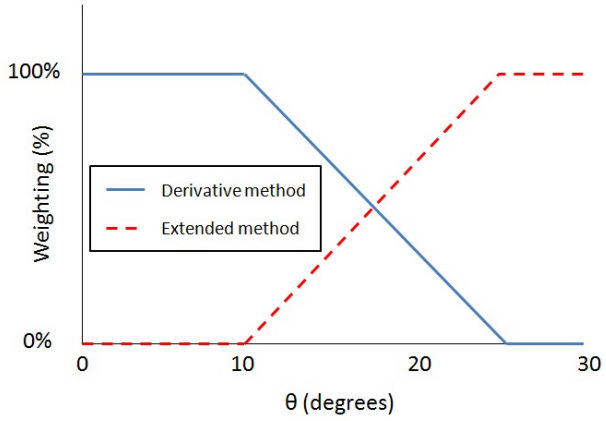

Fig. 7. Method weightings for Fusion Algorithm

The lower and upper switching points are chosen to be 10 and 25 degrees respectively. These values were found to give a smooth transition. These may need changing if the noise levels are considerably different.

The fusion algorithm applies a weighting to each signal based on the value of θ and then outputs the combined total. The output of the fusion algorithm, t_f, can be written as a combination of t_d and t_e, the derivative and extended TPCA method solutions respectively as defined by Equations 8 and 11.

The slope of the line for the extended method in Figure 7 is simply:

$$k = (\theta - c_1)/(c_2 - c_1) \tag{18}$$

Where c_1 and c_2 are the lower and upper switching locations (i.e. $c_1 = 10$ deg. and $c_2 = 25$ deg.). The slope of the line for the derivative method between the upper and lower switching limits is simply $1 - k$.

The fusion algorithm is therefore described by:

$$\begin{array}{c|c} t_f = t_d & \theta \leq c_1^\circ \\ t_f = t_d(1-k) + t_e k & c_1^\circ < \theta < c_2^\circ \\ t_f = t_e & \theta \geq c_2^\circ \end{array} \tag{19}$$

For all simulations Gaussian white noise is added to the switching variable, θ, with a standard deviation of $\sigma = 2^\circ$.

VII. Fusion Algorithm Results

The fusion algorithm is initially tested in two scenarios:

1) Collision Avoidance Scenario, $d_{MIN} = 150m$
2) Separation Assurance Scenario, $d_{MIN} = 1000m$

A. Collision Avoidance Scenario

For this simulation the aircraft are travelling head-on, but the collision is off-set by 150m. $V_A = 50m/s$ $V_B = 50m/s$, $\psi_{\angle AB} = 180^\circ$ and $d_{MIN} = 150m$. The noise levels given in Table I are added to the core variables and the simulation results are given in Figure 8.

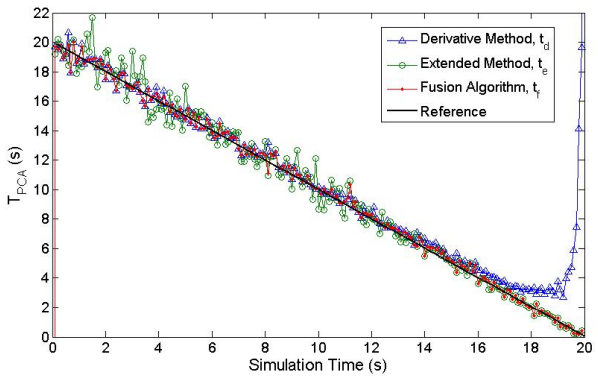

Fig. 8. Fusion algorithm results for low miss distance

It can be seen that the fusion algorithm initially tracks the derivative method when θ is small. As the mathematical assumptions break down, the fusion algorithm accurately switches between the two methods to ensure error is reduced.

B. Large Miss Distance

In this simulation the miss distance is increased to $d_{MIN} = 1000m$. The noise levels remain the same and the results are given in Figure 9.

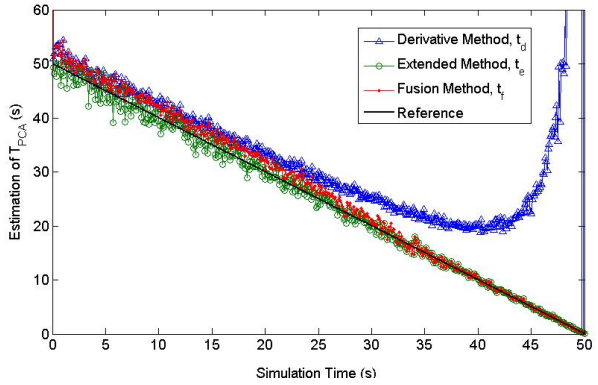

Fig. 9. Fusion algorithm results for high miss distance

It can be seen that for high values of d_{MIN}, the fusion algorithm switches to the extended method much sooner. The extended method is relied upon much more for this type of scenario.

VIII. Limitations

The derivative and extended methods both have limitations. A scenario is set up with a low relative velocity, $V_r = 30m/s$,

where the ownship aircraft approaches the intruder from behind. $V_A = 60m/s$ $V_B = 30m/s$, $\psi_{\angle AB} = 0°$ and $d_{MIN} = 150m$. The results are plotted in Figure 10.

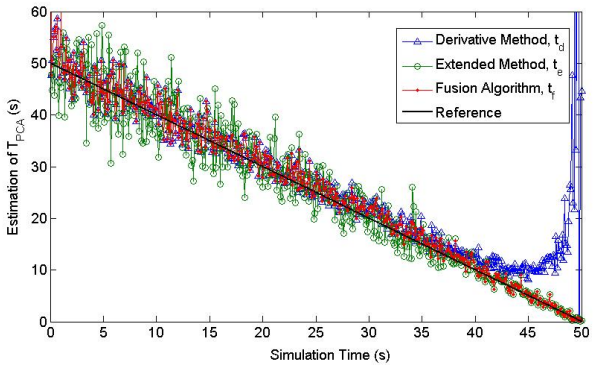

Fig. 10. Fusion algorithm results for low relative velocity

In these low relative velocity scenarios the most obvious difference is the increased noise on both the derivative and extended methods. With further simulations, they were found to get even noisier as the relative velocity between the aircraft, V_r, reduced. Figure 11 shows how the extended method worsens as the relative velocity reduces.

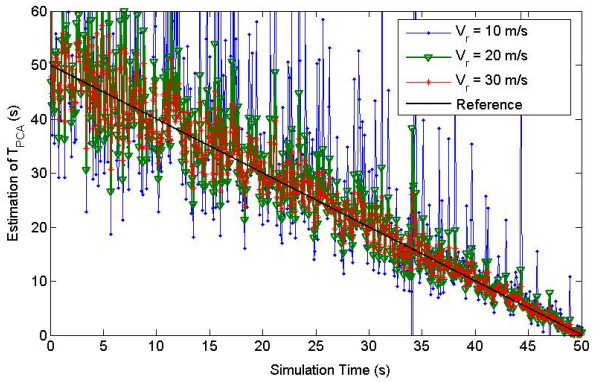

Fig. 11. Extended TPCA estimation method results for a range of relative velocities

This is caused by the uncertainty in V_r overpowering the signal value itself (i.e. Low signal to noise ratio). In reality, clever filtering algorithms would be used to reduce the noise for low relative velocity encounters instead of it being constant. However unless a constant signal to noise ratio could be maintained for low relative velocities, a limit will always be reached where the TPCA estimation becomes unusable.

To overcome the problems with this, TPCA estimations would need to be limited to encounters where the relative velocity was over a certain threshold, defined V_k, that produces an acceptable level of error. The switching points, c_1 and c_2 can then be tuned for this worst case scenario.

Any encounters in which the relative velocity is less than the threshold, $V_r < V_k$, should have their risk defined with another variable, such as the distance to the intruder, d.

IX. Conclusions & Future Work

The derivative methods were derived with limited information on the assumption that the miss distance at the point of closest approach is zero. It was found that as θ increases, the error in the derivative methods increase to a point where they are unusable. An extended method was therefore developed that uses the distance and bearing to the intruder, and their derivatives to calculate the precise TPCA. It was found that for low values of θ the derivative method was superior due to sensor uncertainty propagation being small. The extended method was found to perform much better when θ was large. This is due to the assumptions in the derivative method breaking down to a point where the error they introduce overpowers the uncertainty propagation error from the extended method.

A fusion algorithm was then developed to switch between the two methods, and was found to perform this task well for a range of scenarios with both low and high miss distances. Both the derivative and extended methods were found to deteriorate when the relative velocity V_r was low. This was because of the low signal to noise ratio. To overcome this problem, TPCA would need to be limited in its use to encounters where $V_r > V_k$. Distance could be a better variable to use in low relative velocity encounters as it can be measured directly.

Future work will focus on validating the methods on a small scale UAV using post-processing techniques.

References

[1] CAA, CAP722 - Unmanned Aircraft System Operations in UK Airspace, Guidance

[2] P. Angelov, C. D. Bocaniala, C. Xideas, C. Patchett, D. Ansell, M. Everett and G. Leng, A Passive Approach to Autonomous Collision Detection and Avoidance in Uninhabited Aerial Systems. Tenth International Conference on Computer Modelling and Simulation 2008

[3] A. Martinez, E. Tunstell, and M. Jamshidi, Fuzzy Logic Based Collision Avoidance For a Mobile Robot. Robotica 1994

[4] S. Degen, Reactive image-Based Collision Avoidance System for Unmanned Aircraft Systems. Queensland University of Technology

[5] J. Goss, R. Rajvanshi and K. Subbarao, Aircraft Conflict Detection and Resolution using Mixed Geometric and Collision Cone Approaches. American Institute of Aeronautics and Astronautics

[6] S. Temizer, M. J. Kochenderfer, L. P. Kaelbling, T. Lozano-Perez, and J. K. Kuchar, Unmanned Aircraft Collision Avoidance using Partially-Observable Markov Decision Processes, Massachusetts Institute of Technology, Lincoln Laboratory, Project Report ATC-356, 2009.

[7] W. Schuster and W. Ochieng, Performance requirements of future Trajectory Prediction and Conflict Detection and Resolution tools within SESAR and NextGen: Framework for the derivation and discussion. Journal of Air Transport Management, Volume 35, March 2014, Pages 92101

[8] J. R. Dunthorne, W. H. Chen and S. Dunnett, Collision Avoidance Failure Boundary Identification For The Clearance of Civil Unmanned Aircraft. 2nd Year Internal Report, Loughborough University 2013

[9] R. M. Taylor, Capability, Cognition and Autonomy. RTO HFM Symposium on The Role of Humans in Intelligent and Automated Systems, Warsaw, Poland, Oct 2002

[10] M. J. Kochenderfer, J. K. Kuchar, L. P. Espindle and J.D. Griffith, Uncorrelated Encounter Model of the National Airspace System - Version 1. Project Report, MIT - Lincoln laboratory

[11] D. Eberly, Distance Between Point and Line, Ray, or Line Segment. Geometric Tools (2002)

[12] D. Regan and R. Gray, Visually guided collision avoidance and collision achievement. Trends in Cognitive Sciences Vol. 4, No. 3, March 2000. p99-107 S Degen

[13] S. Widnall, J. Peraire, Lecture L7 - Relative Motion using Translating Axes. 16.07 Dynamics, Fall 2009, Version 2.0